Oxid Met (2018) 89:699–711
https://doi.org/10.1007/s11085-017-9813-6

ORIGINAL PAPER

An XPS Study with Depth Profiling for the Surface Oxide Layer Formed on Aluminides Produced on Superalloy 690 Substrates

R. S. Dutta[1] · Rumu H. Banerjee[1] · G. K. Dey[1]

Received: 20 July 2017 / Revised: 4 October 2017 / Published online: 28 October 2017

Abstract Superalloy 690 substrates containing mainly Cr and Ni aluminides on the uppermost surface, formed by atmospheric plasma spraying and heat treatment, were oxidized at 1273 K in air for 2 h. Quantitative X-ray photoelectron spectroscopy (XPS) analyses indicated that the outermost surface layer formed on aluminides is composed of $\sim$ 21.0 at.% Al^{+3} (as Al_2O_3), 17.0 at.% Al^0 (elemental aluminium), 1.4 at.% Cr^{+3} (as Cr_2O_3) and 60.5 at.% O (in Al_2O_3 and Cr_2O_3 and also includes oxygen contaminant). Surface sputtering for 5 min exhibited splitting of $Cr2p_{3/2}$ peak into a doublet comprising Cr^{+3} (0.9 at.%) and Cr^0 (0.4 at.%) with the presence of 1.15 at.% Ni^0 in the surface layer that mainly contained $\sim$ 37.3 at.% Al^{+3}, 7.3 at.% Al^0 and 52.9 at.% O. Surface sputtering for 15 min indicated surface composition similar to surface sputtered for 5 min but with a marked reduction in ratio of Al^{+3}/Al^0 (32.2 at.% Al^{+3}/11.90 at.% Al^0) in the surface layer.

Keywords Aluminides · Superalloy 690 · Surface oxide · XPS

Introduction

Intermetallic compounds are considered as a topic of research for structural applications at elevated temperatures for the last few decades due to their high melting point, low density (mostly), high resistance to wear and good resistance to aggressive environments at high temperatures [1–7]. In this context, β-NiAl, β-FeAl and Fe_3Al have exhibited promising results [1–3, 8]. Aluminides are known to exhibit superior oxidation resistance that is imparted by an adherent, continuous

✉ R. S. Dutta
rsdutta@barc.gov.in; rsdutta2003@yahoo.com

[1] Materials Science Division, Bhabha Atomic Research Centre, Trombay, Mumbai 400 085, India

Al_2O_3 surface oxide layer, which forms on exposure to air/oxygen environment providing a diffusion barrier coating [9–13]. Better protectiveness of α-Al_2O_3 layer than Cr_2O_3 scale at the temperatures above 1273 K as well as in many aggressive environments having low oxygen partial pressures has also been reported [14, 15]. Various methods, for example, physical/chemical vapour deposition, pack cementation, magnetron sputtering deposition, plasma/laser plasma spraying, are in practice for surface coatings [5, 16–21]. In the present investigation, superalloy 690 substrates containing mainly Cr and Ni aluminides on the uppermost surface, formed by atmospheric plasma spraying and heat treatment, were subjected to thermal oxidation treatment at 1273 K in air for 2 h. This is followed by characterization of surface layer as well as sputtered layers formed on aluminides using quantitative X-ray photoelectron spectroscopy (XPS) technique. This investigation is of prime importance from the perspective of detailed composition analyses of diffusion barrier coatings formed on Ni–Cr–Fe-containing superalloy substrates for high-temperature applications like enhancing service life of metallic melter pots and of electrodes in Joule-heated ceramic melter pot in nuclear waste immobilization process [22–24]. The novelty of the present study lies in the fact that the characterization of Al_2O_3-type oxide (formed on aluminides) that has been done by the investigators [22–24] is predominantly by using X-ray diffraction and microscopic techniques. However, quantitative XPS analyses on Al_2O_3-type surface oxide layer with depth profiling and in addition determination of sputtering yields have not been attempted earlier. This sort of evaluation is of immense importance for complete characterization of diffusion barrier coatings for high-temperature applications.

Experimental Method

Commercially available mill-annealed Ni–Cr–Fe-based superalloy 690 was used as substrates in the present study. The chemical composition of the alloy is given in Table 1. Alloy substrates having dimensions ~ 10 mm × 10 mm × 7 mm were cut from the pipe sample and were solution-annealed at 1373 K for 0.5 h followed by water quenching. The substrates were subjected to atmospheric plasma spraying, followed by standardized heat treatment in air at 1273 K for 3 h to form graded aluminide layers on the alloy substrates. Details of plasma spraying, heat treatment and quantitative scanning electron microscopy with energy-dispersive X-ray spectroscopy (SEM-EDXS) analysis along the cross section have been discussed elsewhere [25]. The alloy substrate containing only the aluminides was thermally oxidized in air at a temperature of 1273 K for 7200 s (2 h) and air-cooled. The XPS

Table 1 The chemical composition of the alloy 690 (wt%)

C	Cr	Fe	Si	Mn	S	Cu	Ni
0.03	28.0	9.6	0.04	0.17	0.001	0.05	Bal

studies on the oxidized specimen were conducted in an electron spectrometer. Al-Kα X-rays ($h\nu = 1486.74$ eV) were used as primary radiation source. The emitted photoelectrons were collected by a hemispherical energy analyser with delay line detector (Phoibos HSA 3500, SPECS). An Ar^+ ion beam of 5 keV with 45 degree incidence was used for sputtering the surface for depth profiling. The XPS spectra were recorded for the as-oxidized surface as well as for the surfaces sputtered for 5 and 15 min. The XPS spectra were recorded for a 2p level of Al, for a $2p_{3/2}$ level of Ni, Cr and Fe and for a 1s level of O and C. The binding energies at the peaks recorded at the photoelectron spectra were corrected with respect to C 1s reference occurring at 284.5 eV. Quantitative elemental analyses were performed using CASA-XPS software with Shirley's background correction. The quantification has been carried out using relative sensitivity factors (RSF) provided in the database of CASA-XPS software. The various RSF factors used are presented in the table given below.

Element	RSF
Al 2p	0.537
Cr 2p	11.7
O 1s	2.93
Ni 2p	22.178

An attempt has also been made to determine approximately the thickness of the sputtered layers using relation of sputtering yield [26–28].

Results

Aluminides

SEM-EDXS analysis along the cross section of plasma-sprayed + heat-treated (1273 K for 3 h) specimen indicated [25] formation of around 50-μm-thick multilayer comprising Cr aluminide + (Ni,Cr)Al-, NiAl- and $(Ni,Cr)_3Al$-type layers and finally, Cr-rich layer adjacent to substrate as shown in Fig. 1.

Qualitative XPS Analyses

As-Oxidized Surface

XPS spectra of aluminium, nickel, chromium and oxygen were recorded for the as-oxidized surface as well as for the surfaces sputtered for 5 and 15 min. The assignments of XPS peaks for the uppermost oxidized surface of aluminides as well as the sputtered ones were made based on rigorous data analyses as well as Gaussian

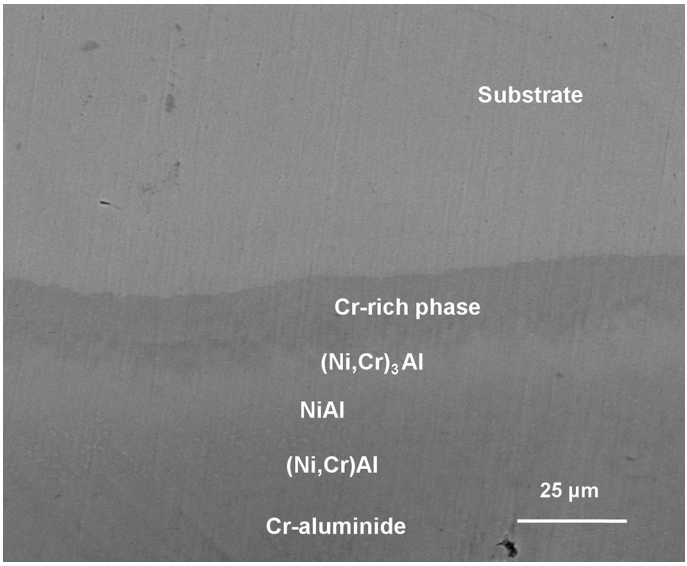

Fig. 1 Formation of multilayer of aluminides along the cross section of plasma-sprayed and heat-treated superalloy 690 substrate

peak fitting model. XPS results for as-oxidized surface revealed that the Al 2p spectrum consists of a doublet. The first Al 2p peak occurred at a binding energy value of 73.1 eV, while the second one was noticed at a value of 74.7 eV indicating the presence of aluminium in the form of elemental aluminium (Al^0) and Al_2O_3 (Al^{+3}), respectively, [29]. In case of $2p_{3/2}$ level of Ni, the peak was obtained at a value of 850.1 eV, which corresponds to a value lower than that of elemental nickel (Ni^0) [30–34]. For $2p_{3/2}$ level of Cr, single peak was recorded at a value of 575.8 eV that corresponds to Cr^{+3} (Cr_2O_3) [32, 35–37]. For O 1 s spectrum, a combined peak was noticed. The first O 1s peak was found to occur at a value of 527.2 eV, and the second one occurred at a value of 529.9 eV corresponding to the presence of oxides of chromium and aluminium [29, 30, 32, 38, 39]. Figure 2a–d demonstrates XPS spectra of aluminium, chromium, nickel and oxygen, respectively, for the as-oxidized surface.

Surface Sputtered for 5 min

After the surface sputtering for 5 min, two peaks were observed for 2p level of Al. The first one was recorded at a value of 73.3 eV and the second one at 75.0 eV indicating the presence of aluminium in the form of Al^0 and Al_2O_3, respectively, [29]. In case of nickel, Ni $2p_{3/2}$ peak was found to occur at a value of 850.4 eV, which corresponds to a value lower than that of elemental nickel [30–34]. For $2p_{3/2}$ level of Cr, two peaks were recorded, one at 572.9 eV and the other at 574.3 eV. These appear to be closely towards Cr^0 and Cr^{+3} (Cr_2O_3), respectively [32, 35–37]. In case of oxygen, the occurrence of O 1s peak was noticed at a value of 530.1 eV

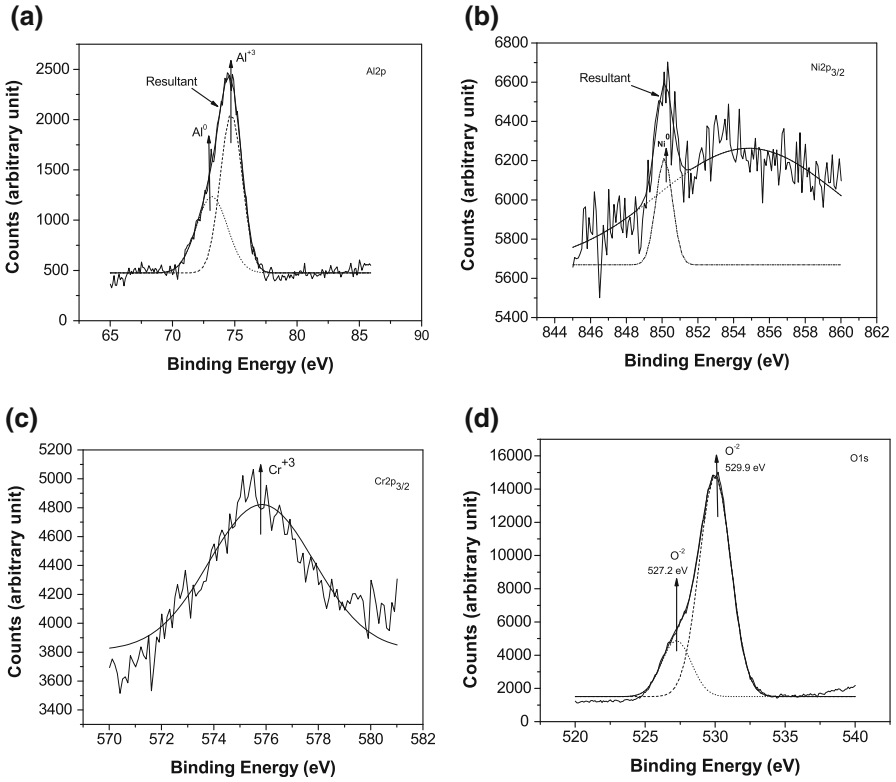

Fig. 2 XPS spectra recorded for **a** Al 2p, **b** Ni $2p_{3/2}$, **c** Cr $2p_{3/2}$ and **d** O 1s for as-oxidized surface of Cr and Ni aluminides formed on superalloy 690 substrate

indicating its presence as oxides of aluminium and chromium [29, 30, 32, 38, 39]. Figure 3a–d shows the XPS spectra of aluminium, chromium, nickel and oxygen, respectively, for the surface that has been sputtered for 5 min.

Surface Sputtered for 15 min

After surface sputtering for 15 min, two peaks were recorded for 2p level of Al those are at the binding energy values of 74.3 and 75.5 eV indicating the presence of elemental aluminium and Al_2O_3 respectively [29]. For nickel, Ni $2p_{3/2}$ peak occurred at a value of 851.2 eV corresponding to a value close to that of elemental nickel [30–34]. For $2p_{3/2}$ level of Cr, two peaks were noticed, one at a binding energy value of 573.8 eV and the other at a value of 575.2 eV corresponding closely to Cr^0 and Cr^{+3} (Cr_2O_3), respectively [32, 35–37]. The O1 s peak was recorded at a value of 530.6 eV indicating its presence as oxides of aluminium and chromium [29, 30, 32, 38, 39]. Figure 4a–d demonstrates XPS spectra of aluminium, chromium, nickel and oxygen, respectively, for the surface that has been sputtered for 15 min. It is evident from the XPS spectra for as-oxidized surface and surfaces sputtered for 5 and 15 min that slight shifts of binding energy values for the

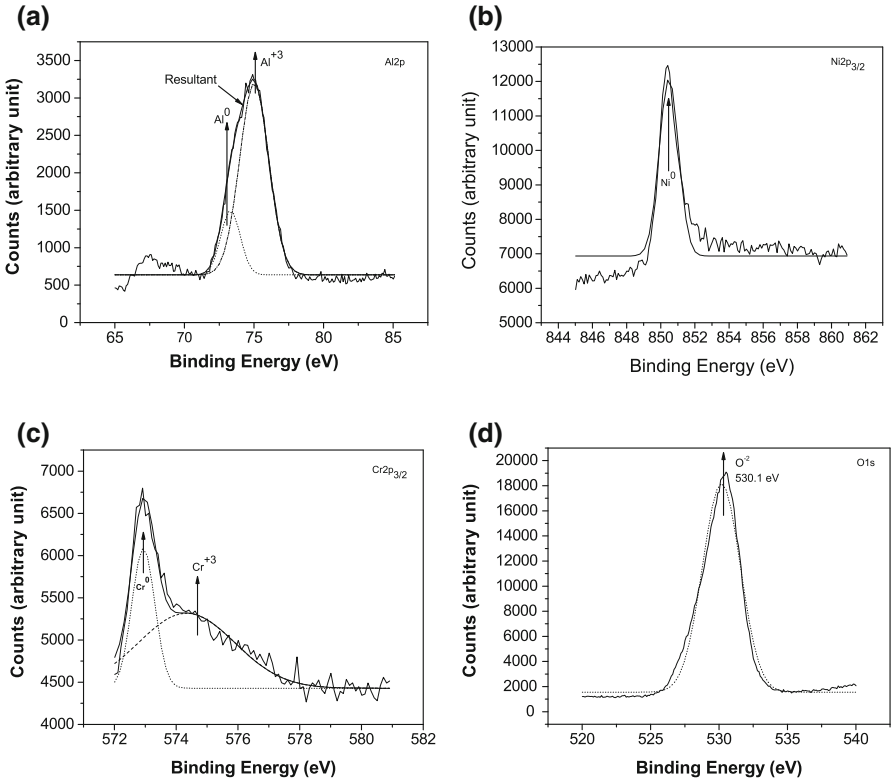

Fig. 3 XPS spectra recorded for **a** Al 2p, **b** Ni $2p_{3/2}$, **c** Cr $2p_{3/2}$ and **d** O 1s for as-oxidized + 5-min sputtered surface of Cr and Ni aluminides formed on superalloy 690 substrate

elements have taken place. The slight shifts in the binding energy values are believed to be mainly attributable to changes in compositions of the oxide layers with sputtering.

Quantitative XPS Analyses

In order to carry out quantitative XPS analyses for the elements, CASA-XPS software was employed on the deconvoluted and peak-fitted XPS spectra for the as-oxidized as well as sputtered surfaces. CASA analyses are based on consideration of standard background (Shirley) noise resulting from inelastically scattered photo-electrons as well as intensity ratio of the elements. The quantitative analyses have been carried out using Voigt fitted peaks. The Voigt peaks contain 30% Lorentzian contribution mainly defining the tail of the peaks. Hence, for qualitative analyses Gaussian fit with straight line background was sufficient since only the peak positions were determined from those while quantitative analyses have been carried out rigorously using Voigt functions showing precise fits. The concentrations thus obtained are accurate up to ± 0.1 at.%. Table 2 shows the results of quantitative XPS analyses for the as-oxidized and sputtered surfaces. It is evident from the

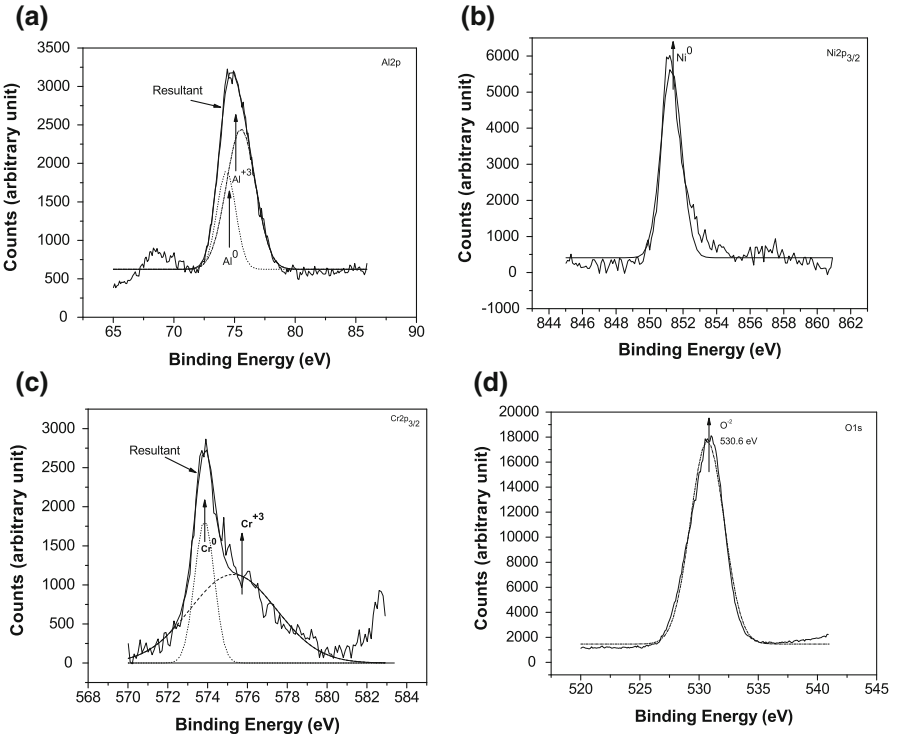

Fig. 4 XPS spectra recorded for **a** Al 2p, **b** Ni $2p_{3/2}$, **c** Cr $2p_{3/2}$ and **d** O 1s for as-oxidized + 15-min sputtered surface of Cr and Ni aluminides formed on superalloy 690 substrate

Table 2 Results of quantitative XPS analyses of surfaces for Cr and Ni aluminides having different surface conditions

Surface condition	Surface compositions, at.%					
	Al^{+3}	Al^{0}	Cr^{+3}	Cr^{0}	Ni^{0}	O
As-oxidized	21.0	17.0	1.4	–	–	60.5
Surface sputtered for 5 min	37.3	7.3	0.9	0.4	1.2	52.9
Surface sputtered for 15 min	32.2	11.9	0.8	0.7	1.2	53.3

results that the as-oxidized surface contains $\sim$ 21.0 at.% Al^{+3}, 17.0 at.% Al^{0}, 1.4 at.% Cr^{+3} and 60.5 at.% O that includes weekly adsorbed oxygen contaminant. The surface sputtered for 5 min has shown surface composition of $\sim$ 37.3 at.% Al^{+3}, 7.3 at.% Al^{0}, 52.9 at.% O, 0.9 at.% Cr^{+3}, 0.4 at.% Cr^{0} and 1.15 at.% Ni^{0} along with an increase in Al^{+3}/Al^{0} ratio. The surface sputtered for 15 min has exhibited surface composition similar to surface sputtered for 5 min but with a reduction in Al^{+3}/Al^{0} ratio.

Determination of Thickness for Sputtered Layers

In order to determine the thickness of the sputtered layers, an attempt has been made to calculate approximately the sputtering rates using sputtering yield relation [26–28]. The calculations are stated as follows:

The sputtering rate is calculated by the formula

$$\dot{Z} = \frac{MSj_p}{\rho \mathrm{Na}e}$$

where $\dot{Z}$ is sputtering rate in Å/min, M, ρ and S are mass, density and sputtering yield, respectively, Na and e are Avogadro number and electronic charge, respectively, and j_p is the ion current density.

The etching/sputtering rate for standard Ta_2O_5 using identical conditions of ion current and Ar ion energy is 50 Å/min and sputtering yield is 21.089 atoms/ion. The sputter rate of the layer in present study is then obtained by

$$\dot{Z} = \left(\frac{MS}{\rho}\right)_{\text{oxide}} * \left(\frac{\rho}{MS}\right)_{Ta_2O_5} * \dot{Z}_{Ta_2O_5}$$

where M and ρ are the effective mass and density, respectively, calculated using the relations

$$\text{Effective mass } M = \sum (\text{atom fraction of component}) * (\text{molar mass of component})$$

$$\text{Effective density} = \text{Effective mass} / \left\{ \sum (\text{mass of component}) / (\text{density of component}) \right\}.$$

The sputtering yield S depends on the atom fraction and atomic number of the components such as Al_2O_3, Cr_2O_3, metallic Ni, metallic Cr, etc., forming the layer and is calculated from the effective atomic number as

$$\text{Effective } Z = \sum (\text{atom fraction of component}) * (\text{atomic number of component}).$$

Table 3 summarizes the values used in the present calculations. Substituting the values, the desired results are obtained as shown in Table 4. It is evident from Table 4 that the sputtering rate decreases after 5 min, which could be attributed to sputter cleaning of the sample. Initially, the weakly adsorbed C and O atoms will get sputtered easily. After sputtering for 5 min, the surface would be clean and the sputtering rate is mainly regulated by the removal of Al_2O_3 layer. High concentration of oxygen in the as-exposed surface as obtained is expected due to the presence of oxide layer. Surface sputtering for 5 min has resulted in removal of substantial amount of adsorbed oxygen indicating a reduction in its concentration. From the calculated sputtering rates, it is evident that these are quite low (< 8 Å/min) and after a sputtering of 15 min a total of $\sim$ 95 Å layer thickness has been removed. The presence of appreciable amount of oxygen after 15 min of sputtering

Table 3 Parameters used during calculations of sputtering rates for the surfaces of Cr and Ni aluminides having different surface conditions

Component	Effective atomic number (*Z*)	Molar mass (g/mol)	Density (kg/m^3)
Al_2O_3	10	101.96	3970
Cr_2O_3	14.5	151.99	5210
Ni	28	58.69	8908
Al	13	26.98	2700
Cr	24	51.996	7140
Ta_2O_5	34	441.89	8200

suggests that the oxide layer is not completely removed by a sputtering duration of 15 min.

Discussion

Atmospheric plasma spraying followed by heat treatment of superalloy 690 substrates has resulted in formation of multilayer comprising Cr and Ni aluminides on the uppermost surface and Ni aluminides with varying Al contents as adjoining layers as shown in Fig. 1. The formation of multilayer has received detailed discussion in earlier paper [25]. The formation of multilayer is postulated [25] by inward diffusion of aluminium and outward diffusion of alloying elements. At the initial stage, high aluminium content on the alloy surface appeared to have led to the formation of Cr aluminide along with Ni aluminide. At the later stage, it was the outward diffusion of aluminium that seemed to be the predominant process as the area adjacent to substrate exhibited Cr-rich phase similar to mechanism of formation of NiAl layer for low-aluminium-containing pack aluminizing process.

Thermal oxidation of Cr and Ni aluminides formed on superalloy 690 substrates has exhibited formation of surface oxide layer. Quantitative XPS analyses along with depth profiling have indicated that the outermost surface layer formed on aluminides is comprising $\sim$ 21.0 at.% Al^{+3} (as Al_2O_3), 17.0 at.% Al^0 (elemental aluminium), 1.4 at.% Cr^{+3} (as Cr_2O_3) and 60.5 at.% O (in Al_2O_3 and Cr_2O_3 and also includes oxygen contaminant). Surface sputtering for 5 min has shown splitting of $Cr2p_{3/2}$ peak into a doublet consisting of Cr^{+3} (0.9 at.%) and Cr^0 (0.4 at.%) with the presence of 1.15 at.% Ni^0 in the surface layer that mainly contained $\sim$ 37.3 at.% Al^{+3}, 7.3 at.% Al^0 and 52.9 at.% O. An increase in the ratio of Al^{+3}/Al^0 for the surface sputtered for 5 min as compared to the as-oxidized one could be attributable to surface cleaning phenomenon. Surface sputtering for 15 min has exhibited surface composition similar to surface sputtered for 5 min but with a marked reduction in ratio of Al^{+3}/Al^0 (32.2 at.% Al^{+3}/11.9 at.% Al^0) in the surface layer. The calculations on sputtering yields for the surface layers have indicated a sputtering rate in the vicinity of 7 Å/min for the as-oxidized surface and 5.9 Å/min for the surface sputtered for 5 min resulting in removal of approximately 35 and

Table 4 Results on sputtering rates and thicknesses of the layers removed for the surfaces of Cr and Ni aluminides having different surface conditions

Initial surface condition	Effective atomic number (Z)	Effective density (Kg/m^3)	Sputtering yield	Sputtering rate (Å/min)	Sputtering duration (min)	Layer thickness removed with the sputter rate (Å)	Total thickness removed (Å)
As-oxidized surface	11	4120.9	6.89	7.1(± 0.06)	5	35.6(± 0.3)	35.6
Surface sputtered for 5 min	11	5380.1	6.89	5.9(± 0.07)	10	59.3(± 0.7)	94.9

95 Å thicknesses of layers after surface sputtering for 5 and 15 min, respectively. The findings of low overall sputtering rates of surface oxide layers as obtained in the present investigation that could be attributable to the presence of primarily Al_2O_3-type oxide appear to be in accordance with the results of other investigators [27].

The oxidation behaviour of NiAl and phase transformation of surface oxide layer formed on nickel aluminide during high-temperature oxidation have been examined by a few investigators [40–43]. Brumm and Grabke have examined the oxide layer that formed on NiAl and NiAl-Cr alloys after an oxidation treatment of about 300 h in oxygen + helium environment at 1273 K. The characterization of the oxide layer has been performed using X-ray diffraction (XRD) technique as well as transmission electron microscope (TEM). The authors have reported that the surface oxide is of α-Al_2O_3 type [40]. The oxidation behaviour of β-NiAl layer, prepared on Ni-based superalloy substrate, has been studied by Liu et al. [41] at 1223 K in air. The authors have characterized the oxide layer employing glancing-angle XRD technique and TEM. The investigators [41] have observed transformation of most of the grains of θ-Al_2O_3 into α-Al_2O_3 after an oxidation treatment for 3 h. It is also reported by Choi et al. [42] that the surface oxide layer that formed on β-NiAl in air at 1373 K for a period of 6 h is primarily composed of α-Al_2O_3 containing a very little trace of θ-Al_2O_3. The authors have used glancing-angle XRD technique and TEM while characterizing the oxide. According to Dutta et al. [24], thermal oxidation at 1273 K for 4 h in air of (NiCr)Al + Cr_5Al_8-type aluminides, formed by pack aluminization on superalloy 690 substrates, has indicated formation of Al_2O_3-type surface oxide layer as revealed by scanning electron microscope with energy-dispersive X-ray spectroscopy (SEM–EDS) analysis. Investigation by Jaeger et al. [43] focusses on evaluation of characteristics of thin film of Al_2O_3 epitaxially grown on NiAl (110). The authors [43] have employed XPS and auger electron spectroscopy (AES) techniques along with the other like low-energy electron diffraction (LEED) and electron energy loss spectroscopy (EELS) to examine the thin Al_2O_3 film. XPS with AES analyses with deconvolution has clearly indicated the presence of Al^{+3}(as Al_2O_3) having a thickness of 5 Å. According to their [43] findings, LEED data indicate that Al_2O_3 film contains distorted hexagonal oxygen layer, while EELS results lead to the suggestion that the structure of the oxide film is similar to that of γ-Al_2O_3 or α-Al_2O_3. It is, therefore, indicative of the fact that the formation of predominantly Al_2O_3-type surface oxide layer on Cr and Ni aluminides as observed in the present study is in agreement with the results of other investigators, and the alumina is believed to be of α-Al_2O_3 type [24, 40–42].

Conclusions

The outermost surface layer formed by oxidation on Cr and Ni aluminides produced by plasma spraying and heat treatment of superalloy 690 substrates is mainly composed of Al_2O_3-type oxide layer with some amount of elemental aluminium and very little Cr^{+3} (as Cr_2O_3). Depth profiling up to around 35 Å thickness has indicated the presence of very small amounts of elemental chromium, elemental nickel also in the inner layer along with the increase of Al^{+3}/Al^0 ratio that could be

attributable to surface cleaning phenomenon. Depth profiling up to 95 Å thickness has shown surface composition similar to 35 Å sputtered surface but with a marked reduction in Al^{+3}/Al^{0} ratio. The surface layers exhibit low sputtering rate.

Acknowledgements The work has been funded by Department of Atomic Energy, Government of India.

References

1. S. C. Deevi and V. K. Sikka, *Intermetallics* **4**, 357 (1996).
2. N. S. Stoloff, *Materials Science and Engineering A* **258**, 1 (1998).
3. R. S. Sundar, R. C. Balligidad, Y. V. R. K. Prasad, and D. H. Sastry, *Materials Science and Engineering A* **258**, 219 (1998).
4. G. W. Goward, *Surface and Coating Technology* **108–109**, 73 (1998).
5. C. Houngnlou, S. Chavaller, and J. P. Larpin, *Applied Surface Science* **236**, 256 (2004).
6. R. A. Mahesh, R. Jayaganthan, and S. Prakash, *Surface Engineering* **26**, 413 (2010).
7. R. S. Dutta, A. Arya, C. Yusufali, B. Vishwanadh, R. Tewari, and G. K. Dey, *Surface and Coating Technolgy* **235**, 741 (2013).
8. J. Xia, C. X. Li, and H. Dong, *Wear* **258**, 1804 (2005).
9. D. Li, Y. Xu, and D. Lin, *Journal of Materials Science* **36**, 979 (2001).
10. Z. D. Xiang, S. R. Rose, and P. K. Datta, *Scripta Materialia* **59**, 99 (2008).
11. H. Guoxin, X. Zhengxia, I. Jianju, and I. Yanhong, *Surface and Coating Technolgy* **203**, 3392 (2009).
12. M. A. Espinosa-Madina, G. Carbajal-Dela Torre, H. B. Liu, A. Martińez-Villafañe, and J. G. González-Rodriguez, *Corrosion Science* **51**, 1420 (2009).
13. S. Kamal, R. Jayaganthan, and S. Prakash, *Surface Engineering* **26**, 453 (2010).
14. J. Klöwer, U. Brill, and U. Heubner, *Intermetallics* **7**, 1183 (1999).
15. H. Cho and B. W. Lee, *Modern Physics Letters B* **29**, 1 (2015).
16. V. Chaturvedi, P. V. Ananthapadmanabhan, Y. Chakravarthy, S. Bhandari, N. Tiwari, A. Pragatheeswaran, and A. K. Das, *Ceramics International* **40**, 8273 (2014).
17. T. K. Thiyagarajan, P. V. Ananthapadmanabhan, K. P. Sreekumar, Y. Chakravarthy, A. K. Das, L. M. Gantayet, B. Selvan, and K. Ramachandran, *Surface Engineering* **28**, 646 (2012).
18. D. Thirumalaikumarasamy, K. Shanmugam, and V. Balasubramanian, *Surface Engineering* **28**, 759 (2012).
19. Q. Y. Chen, C. X. Li, J. Z. Zhao, G. J. Yang, and C. J. Li, *Materials and Manufacturing Processes* **31**, 1183 (2016).
20. E. M. Stanciu, A. Pascu, M. H. Ţierean, I. Voiculescu, I. C. Roată, C. Croitoru, and I. Hulka, *Materials and Manufacturing Processes* **31**, 1556 (2016).
21. M. R. Bateni, S. Shaw, P. Wei, and A. Petric, *Materials and Manufacturing Processes* **24**, 626 (2009).
22. K. Raj, K. K. Prasad, and N. K. Bansal, *Nuclear Engineering Design* **236**, 914 (2006).
23. R.S. Dutta, in Book *Corrosion Research Trends*, *Chapter 11*, ed. I.S. Wang (Nova Science Publishers, Inc. New York, 2007), p. 349.
24. R. S. Dutta, C. Yusufali, B. Paul, S. Majumdar, P. Sengupta, R. K. Mishra, C. P. Kaushik, R. J. Khirsagar, U. D. Kulkarni, and G. K. Dey, *Journal Nuclear Materials* **432**, 72 (2013).
25. R.S. Dutta, S. Bhandari, Y. Chakravarthy, B. Vishwanadh, K. Singh, and G.K. Dey, in *Materials Today: Proceedings (ARRMA 2016)*, vol. 3, ed. S. Majumdar (Elsevier 2016), p. 3018.
26. S. Hofmann, *Surface and Interface Analysis* **2**, 148 (1980).
27. H. Viefhaus, K. Hennessen, M. Lucas, E. M. Müller-Lorenz, and H. J. Grabke, *Surface and Interface Analysis* **21**, 665 (1994).
28. M. P. Seah and T. S. Nnney, *Journal of Physics D: Applied Physics* **43**, 253001 (2010).
29. C. D. Wagner, W. M. Riggs, L. E. Davis, J. F. Moulder, and G. E. Muilenberg, *Handbook of X-ray Photoelectron Spectroscopy*, (Perkin-Elmer Corporation, Eden prairie, Minnesota, 1979).
30. R. S. Dutta, Jagannath, G. K. Dey, and P. K. De, *Corrosion Science* **48**, 2711 (2006).
31. R. S. Dutta, R. Purandare, A. Lobo, S. K. Kulkarni, and G. K. Dey, *Corrosion Science* **46**, 2937 (2004).

32. R. S. Dutta, A. Lobo, R. Purandare, S. K. Kulkarni, and G. K. Dey, *Metallurgical and Materials Transactions A* **33A**, 1437 (2002).
33. P. Marcus and J.-M. Herbalin, *Corrosion Science* **34**, 1123 (1993).
34. G. K. Dey, R. T. Savalia, S. K. Sharma, and S. K. Kulkarni, *Corrosion Science* **29**, 823 (1989).
35. P. Marcus and J. M. Grimal, *Corrosion Science* **33**, 805 (1992).
36. B. Stypula and J. Stoch, *Corrosion Science* **36**, 2159 (1994).
37. N. S. McIntyre, D. G. Zetaruk, and D. Owen, *Journal of Electrochemical Society* **126**, 750 (1979).
38. I. Olefjord, B. Brox, and U. Jelvestam, *Journal of Electrochemical Society* **132**, 2854 (1985).
39. P. Marcus and I. Olefjord, *Corrosion* **42**, 91 (1986).
40. M. W. Brumm and H. J. Grabke, *Corrosion Science* **33**, 1677 (1992).
41. G. Liu, M. Li, M. Zhu, and Y. Zhou, *Intermetallics* **15**, 1285 (2007).
42. H. J. Choi, J. Jedlinski, B. Yao, and Y. H. Shon, *Surface and Coating Technolgy* **205**, 1206 (2010).
43. R. M. Jaeger, H. Kuhlenbeck, H.-J. Freund, M. Wittig, W. Hoffmann, R. Franchy, and H. Ibach, *Surface Science* **259**, 235 (1991).